

## RESEARCH ARTICLE SUMMARY

## HUMAN GENOMICS

## Cell type–specific genetic regulation of gene expression across human tissues

Sarah Kim-Hellmuth\*, François Aguet, Meritxell Oliva, Manuel Muñoz-Aguirre, Silva Kasela, Valentin Wucher, Stephane E. Castel, Andrew R. Hamel, Ana Viñuela, Amy L. Roberts, Serghei Mangul, Xiaoquan Wen, Gao Wang, Alvaro N. Barbeira, Diego Garrido-Martín, Brian B. Nadel, Yuxin Zou, Rodrigo Bonazzola, Jie Quan, Andrew Brown, Angel Martínez-Perez, José Manuel Soria, GTEx Consortium, Gad Getz, Emmanouil T. Dermitzakis, Kerrin S. Small, Matthew Stephens, Hualin S. Xi, Hae Kyung Im, Roderic Guigó, Ayellet V. Segrè, Barbara E. Stranger, Kristin G. Ardlie, Tuuli Lappalainen\*

**INTRODUCTION:** Efforts to map quantitative trait loci (QTLs) across human tissues by the GTEx Consortium and others have identified expression and splicing QTLs (eQTLs and sQTLs, respectively) for a majority of genes. However, these studies were largely performed with gene expression measurements from bulk tissue samples, thus obscuring the cellular specificity of genetic regulatory effects and in turn limiting their functional interpretation. Identifying the cell type (or types) in which a QTL is active will be key to uncovering the molecular mechanisms that underlie complex trait variation. Recent studies demonstrated the feasibility of identifying cell type–specific QTLs from bulk tissue RNA-sequencing data by using computational estimates of cell type proportions. To date, such approaches have only been applied to a limited number of cell types and tissues. By applying this methodology to GTEx tissues for a diverse set of cell types, we aim to characterize the cellular specificity of genetic effects across human tissues and to describe the contribution of these effects to complex traits.

**RATIONALE:** A growing number of in silico cell type deconvolution methods and associated reference panels with cell type–specific marker genes enable the robust estimation of the enrichment of specific cell types from bulk tissue gene expression data. We benchmarked and used enrichment estimates for seven cell types (adipocytes, epithelial cells, hepatocytes, keratinocytes, myocytes, neurons, and neutrophils) across 35 tissues from the GTEx project to map QTLs that are specific to at least one cell type. We mapped such cell type–interaction QTLs for expression and splicing (ieQTLs and isQTLs, respectively) by testing for interactions between genotype and cell type enrichment.

**RESULTS:** Using 43 pairs of tissues and cell types, we found 3347 protein-coding and long intergenic noncoding RNA (lincRNA) genes with an ieQTL and 987 genes with an isQTL (at 5% false discovery rate in each pair). To validate these findings, we tested the QTLs for replication in available external datasets and

applied an independent validation using allele-specific expression from eQTL heterozygotes. We analyzed the cell type–interaction QTLs for patterns of tissue sharing and found that ieQTLs are enriched for genes with tissue-specific eQTLs and are generally not shared across unrelated tissues, suggesting that tissue-specific eQTLs originate in tissue-specific cell types. Last, we tested the ieQTLs and isQTLs for colocalization with genetic associations for 87 complex traits. We show that cell type–interaction QTLs are enriched for complex trait associations and identify colocalizations for hundreds of loci that were undetected in bulk tissue, corresponding to an increase of >50% over colocalizations with standard QTLs. Our results also reveal the cellular specificity and potential origin for a similar number of colocalized standard QTLs.

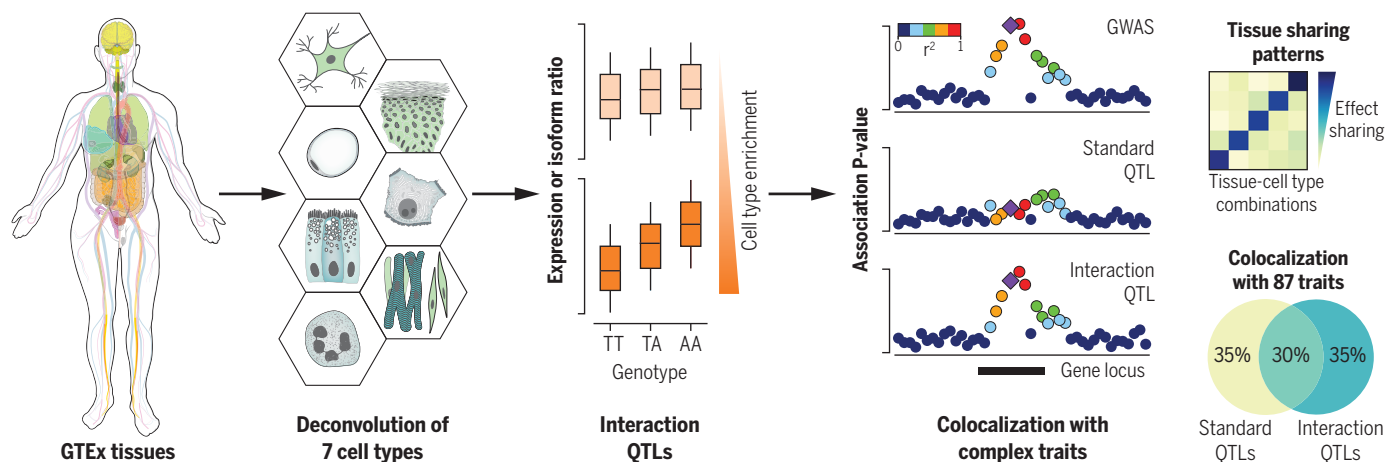
**CONCLUSION:** The ieQTLs and isQTLs identified for seven cell types across GTEx tissues suggest that the large majority of cell type–specific QTLs remains to be discovered. Our colocalization results indicate that comprehensive mapping of cell type–specific QTLs will be highly valuable for gaining a mechanistic understanding of complex trait associations. We anticipate that the approaches presented here will complement studies mapping QTLs in single cells. ■

The list of author affiliations and a full list of the GTEx authors and their affiliations are available in the full article online.

\*Corresponding author. Email: skimhellmuth@gmail.com (S.K.-H.); tlappalainen@nygenome.org (T.L.)

Cite this article as S. Kim-Hellmuth *et al.*, *Science* 369, eaaz8528 (2020). DOI: 10.1126/science.aaz8528

**S** READ THE FULL ARTICLE AT <https://doi.org/10.1126/science.aaz8528>



**Detection of cell type–specific effects on gene expression.** The enrichment of seven cell types is calculated across GTEx tissues, enabling mapping of cell type–interaction QTLs for expression and splicing by testing for significant interactions between genotypes and cell type enrichments. Linking these QTLs to complex trait associations enables discovery of >50% more colocalizations compared with standard QTLs and reveals the cellular specificity of traits.

## RESEARCH ARTICLE

## HUMAN GENOMICS

## Cell type-specific genetic regulation of gene expression across human tissues

Sarah Kim-Hellmuth<sup>1,2,3\*</sup>†‡, François Aguet<sup>4</sup>†, Meritxell Oliva<sup>5,6</sup>, Manuel Muñoz-Aguirre<sup>7,8</sup>, Silva Kasela<sup>2,3</sup>, Valentin Wucher<sup>7</sup>, Stephane E. Castel<sup>2,3</sup>, Andrew R. Hamel<sup>4,9</sup>, Ana Viñuela<sup>10,11,12,13</sup>, Amy L. Roberts<sup>10</sup>, Serghei Mangui<sup>14,15</sup>, Xiaoquan Wen<sup>16</sup>, Gao Wang<sup>17</sup>, Alvaro N. Barbeira<sup>5</sup>, Diego Garrido-Martín<sup>7</sup>, Brian B. Nadel<sup>18</sup>, Yuxin Zou<sup>19</sup>, Rodrigo Bonazzola<sup>5</sup>, Jie Quan<sup>20</sup>, Andrew Brown<sup>11,21</sup>, Angel Martinez-Perez<sup>22</sup>, José Manuel Soria<sup>22</sup>, GTEx Consortium<sup>§</sup>, Gad Getz<sup>4,23,24</sup>, Emmanouil T. Dermitzakis<sup>11,12,13</sup>, Kerrin S. Small<sup>10</sup>, Matthew Stephens<sup>17</sup>, Hualin S. Xi<sup>25</sup>, Hae Kyung Im<sup>5</sup>, Roderic Guigo<sup>7,26</sup>, Ayellet V. Segre<sup>4,9</sup>, Barbara E. Stranger<sup>5,27</sup>, Kristin G. Ardlie<sup>4</sup>, Tuuli Lappalainen<sup>2,3,\*</sup>

The Genotype-Tissue Expression (GTEx) project has identified expression and splicing quantitative trait loci in cis (QTLs) for the majority of genes across a wide range of human tissues. However, the functional characterization of these QTLs has been limited by the heterogeneous cellular composition of GTEx tissue samples. We mapped interactions between computational estimates of cell type abundance and genotype to identify cell type–interaction QTLs for seven cell types and show that cell type–interaction expression QTLs (eQTLs) provide finer resolution to tissue specificity than bulk tissue cis-eQTLs. Analyses of genetic associations with 87 complex traits show a contribution from cell type–interaction QTLs and enables the discovery of hundreds of previously unidentified colocalized loci that are masked in bulk tissue.

The Genotype-Tissue Expression (GTEx) project (1) and other studies (2–5) have shown that genetic regulation of the transcriptome is widespread. The GTEx Consortium in particular has built an extensive catalog of expression and splicing quantitative trait loci in cis (cis-eQTLs and cis-sQTLs, respectively) across a large range of tissues, showing that these cis-eQTLs and cis-sQTLs (collectively referred to here as QTLs) are generally either highly tissue specific or widely shared, even across dissimilar tissues and organs (1, 6). However, the majority of these studies have been performed by using heterogeneous bulk tissue samples comprising diverse cell types. This limits the power, interpretation, and downstream applications of QTL studies. Genetic effects that are active only in rare cell types within a sampled tissue may be undetected, a mechanistic interpretation of QTL sharing across tissues and other contexts is complicated without understanding differ-

ences in cell type composition, and inference of downstream molecular effects of regulatory variants without the specific cell type context is challenging. Efforts to map eQTLs in individual cell types have been largely restricted to blood, using purified cell types (7–11) or single-cell sequencing (12).

Although there are many ongoing efforts to optimize single-cell and single-nucleus sequencing of human tissues (13, 14), including as part of the Human Cell Atlas (15), these methods are not yet scalable to sample sizes and coverage sufficient to achieve power comparable with that of bulk eQTL studies (16–18). However, cell type-specific eQTLs can be computationally inferred from bulk tissue measurements by using estimated proportions or enrichments of relevant cell types to test for interactions with genotype. To date, such approaches have only been applied to a limited range of cell types, such as blood cells (19, 20) and adipocytes (21). These studies identified thousands of cell type

interactions in eQTLs discovered in whole-blood samples from large cohorts [5683 samples, (19); 2116 samples, (20)], indicating that large numbers of interactions are likely to be identified by expanding this type of analysis to other tissues and cell types.

## Identifying cell types in silico in bulk tissue

We used computational estimates of cell type enrichment to characterize the cell type specificity of cis-eQTLs and cis-sQTLs for 43 cell type–tissue combinations, using seven cell types across 35 tissues (Fig. 1A). Estimating the cell type composition of a tissue biospecimen from RNA-sequencing (RNA-seq) remains a challenging problem (22), and multiple approaches for inferring cell type proportions have been proposed (23). We performed extensive benchmarking for multiple cell types across several expression datasets (figs. S1 and S2). The xCell method (24), which estimates the enrichment of 64 cell types using reference profiles, was most suitable on the combined basis of correlation with cell counts in blood (fig. S1A), in silico simulations (fig. S1B), correlation with expression of marker genes for each cell type (fig. S1, C and D), and diversity of reference cell types. Concordance between methods was generally high (fig. S1, A and E). Furthermore, the inferred abundances reflected differences in histology (fig. S1C) and tissue pathologies (fig. S2). For each cell type, we selected tissues where the cell type was highly enriched (fig. S3). The xCell scores for these tissue–cell type pairs were highly correlated with the probabilistic estimation of expression residuals (PEER) factors used to correct for unobserved confounders in the expression data for QTL mapping (fig. S4A) (1) but were generally weakly correlated with known technical confounders (fig. S4B), suggesting that cell type composition accounts for a large fraction of intersample variation in gene expression.

## Mapping cell type–interaction eQTLs and sQTLs

To identify cis-eQTLs and cis-sQTLs whose effect varies depending on the enrichment of the cell type, we leveraged the variability in cell type composition across GTEx samples

<sup>1</sup>Statistical Genetics, Max Planck Institute of Psychiatry, Munich, Germany. <sup>2</sup>New York Genome Center, New York, NY, USA. <sup>3</sup>Department of Systems Biology, Columbia University, New York, NY, USA. <sup>4</sup>The Broad Institute of MIT and Harvard, Cambridge, MA, USA. <sup>5</sup>Section of Genetic Medicine, Department of Medicine, University of Chicago, Chicago, IL, USA. <sup>6</sup>Department of Public Health Sciences, University of Chicago, Chicago, IL, USA. <sup>7</sup>Centre for Genomic Regulation (CRG), The Barcelona Institute for Science and Technology, Barcelona, Catalonia, Spain. <sup>8</sup>Department of Statistics and Operations Research, Universitat Politècnica de Catalunya (UPC), Barcelona, Catalonia, Spain. <sup>9</sup>Ocular Genomics Institute, Massachusetts Eye and Ear, Harvard Medical School, Boston, MA, USA. <sup>10</sup>Department of Twin Research and Genetic Epidemiology, King's College London, London, UK. <sup>11</sup>Department of Genetic Medicine and Development, University of Geneva Medical School, Geneva, Switzerland. <sup>12</sup>Institute for Genetics and Genomics in Geneva (iGE3), University of Geneva, Geneva, Switzerland. <sup>13</sup>Swiss Institute of Bioinformatics, Geneva, Switzerland. <sup>14</sup>Department of Computer Science, University of California, Los Angeles, Los Angeles, CA, USA. <sup>15</sup>Department of Clinical Pharmacy, School of Pharmacy, University of Southern California, Los Angeles, Los Angeles, CA, USA. <sup>16</sup>Department of Biostatistics, University of Michigan, Ann Arbor, MI, USA. <sup>17</sup>Department of Human Genetics, University of Chicago, Chicago, IL, USA. <sup>18</sup>Department of Molecular, Cellular, and Developmental Biology, University of California, Los Angeles, Los Angeles, CA, USA. <sup>19</sup>Department of Statistics, University of Chicago, Chicago, IL, USA. <sup>20</sup>Inflammation & Immunology, Pfizer, Cambridge, MA, USA. <sup>21</sup>Population Health and Genomics, University of Dundee, Dundee, Scotland, UK. <sup>22</sup>Unit of Genomic of Complex Diseases, Institut d'Investigació Biomèdica Sant Pau (IIB-Sant Pau), Barcelona, Spain. <sup>23</sup>Cancer Center and Department of Pathology, Massachusetts General Hospital, Boston, MA, USA. <sup>24</sup>Harvard Medical School, Boston, MA, USA. <sup>25</sup>Foundational Neuroscience Center, AbbVie, Cambridge, MA, USA. <sup>26</sup>Universitat Pompeu Fabra (UPF), Barcelona, Catalonia, Spain. <sup>27</sup>Center for Genetic Medicine, Department of Pharmacology, Northwestern University, Feinberg School of Medicine, Chicago, IL, USA.

\*Corresponding author. Email: skimhellmuth@gmail.com (S.K.-H.); tlappalainen@nygenome.org (T.L.) †These authors contributed equally to this work. ‡Present address: Department of Pediatrics, Dr. von Hauner Children's Hospital, University Hospital LMU Munich, Munich, Germany. §A full list of the GTEx authors and their affiliations is available at the end of this article.

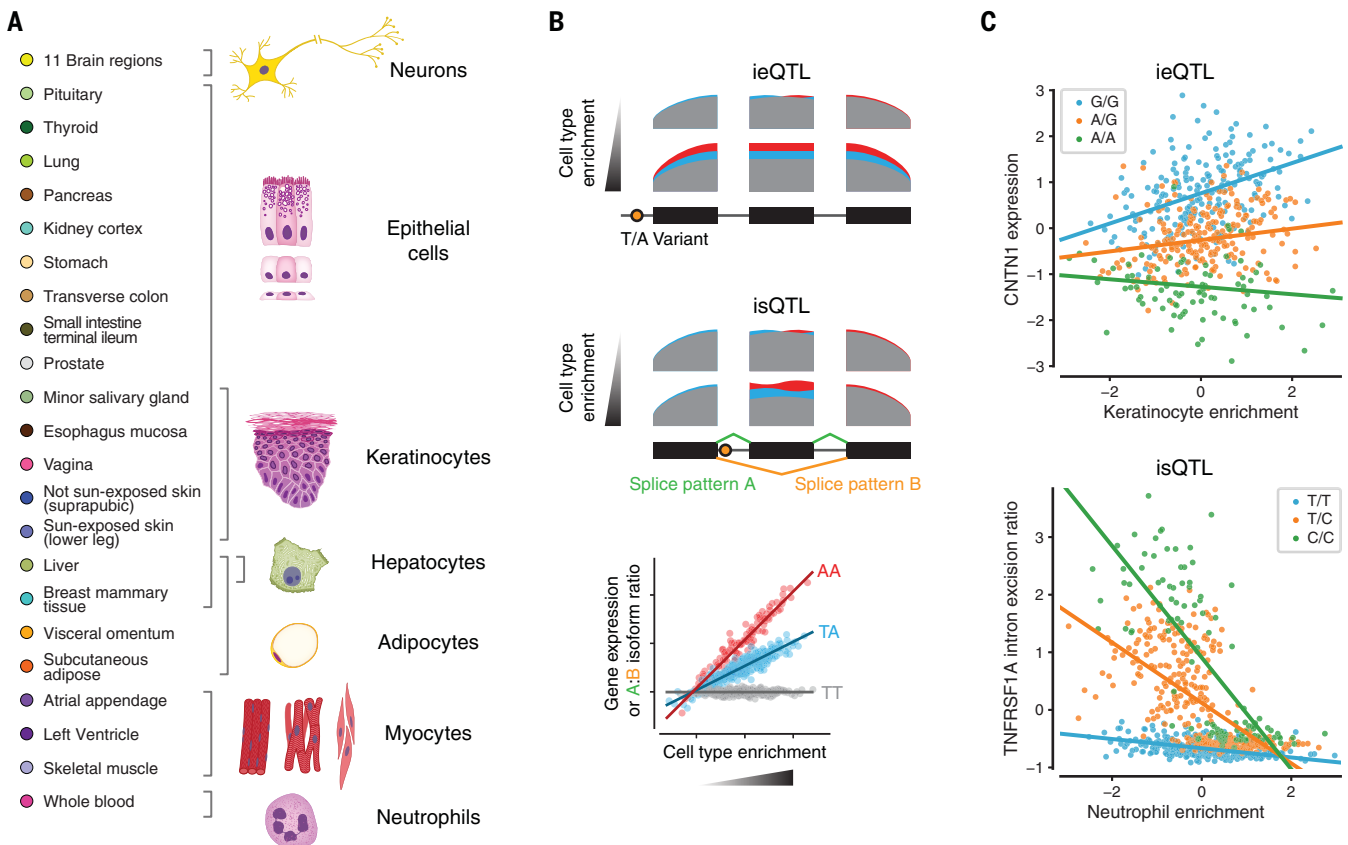


**Fig. 1. Study design of mapping cell type ieQTLs and isQTLs in this study.**

(A) Illustration of 43 cell type–tissue pairs included in the GTEx v8 project. The full list of tissues included in the GTEx v8 project is provided in (1); two brain regions (frontal cortex and cerebellum) were sampled in replicates. Cell types with median xCell enrichment score >0.1 within a tissue were used (fig. S2). (B) Schematic representation of a cell type–interaction eQTL and sQTL. RNA-seq coverage is depicted in gray, blue, and red, representing different genotypes. Differences in coverage between genotypes, corresponding to a QTL effect, are only observed with high cell type enrichment. The scatter plot illustrates the regression model used to identify iQTLs, where

the dots indicate individual samples. (C) Example cell type ieQTL and isQTL. (Top) The *CNTN1* eQTL effect in skin unexposed to the Sun is associated with keratinocyte abundance ( $P = 4.1 \times 10^{-19}$ ). (Bottom) The *TNFRSF1A* sQTL effect in whole blood is associated with neutrophil abundance but is only detected in samples with lower neutrophil abundances ( $P = 6.7 \times 10^{-78}$ ). Each data point represents an individual and is colored by genotype. Cell type enrichment scores and gene expression were inverse normal transformed, and intron excision ratios were standardized. The regression lines from the interaction model illustrate how the QTL effect is modulated by cell type enrichment.

to test for an interaction between cell type and genotype using a linear regression model for either gene expression or splicing (Fig. 1, B and C, and fig. S5, A and B) (25). Because QTLs identified this way are not necessarily specific to the estimated cell type but may reflect another correlated (or anticorrelated) cell type, we refer to these eQTLs and sQTLs as cell type–interaction eQTLs (ieQTLs) and cell type–interaction sQTLs (isQTLs), respectively (or iQTLs in aggregate).

Across cell types and tissues, we detected 3347 protein coding and long intergenic non-coding RNA (lincRNA) genes with an ieQTL [ieGenes (26)] and 987 genes with an isQTL (isGenes) at 5% false discovery rate (FDR) per cell type–tissue combination (Fig. 2A, figs. S5C and S6, and table S1). In the following analyses, we used ieQTLs and isQTLs identified with 5% FDR unless indicated otherwise. Whereas 85% of ieQTLs corresponded to genes with at

least one standard cis-eQTL [eGenes; we refer to cis-eQTLs mapped in bulk tissue as standard eQTLs for simplicity (26)], 21% of these ieQTLs were not in linkage disequilibrium (LD) [coefficient of determination ( $R^2$ ) < 0.2] with any of the corresponding eGene's conditionally independent eQTLs (fig. S7, A and B) (1). For comparison, the proportion of genes with at least one standard eQTL varies as a function of sample size (1), with a median of 42% across tissues (48% in transverse colon and 63% in whole blood). This indicates that ieQTL analysis frequently reveals genetic regulatory effects that are not detected with standard eQTL analysis of heterogeneous tissue samples. Unlike standard cis-QTL discovery, ieQTL discovery was only modestly correlated with sample size (Spearman's  $\rho = 0.53$  and 0.35, for ieQTLs and isQTLs, respectively) (fig. S7, C and D). The tissues with most iQTLs included blood, as well as transverse colon and

breast, which both stratified into at least two distinct groups on the basis of histology (27): epithelial versus adipose tissue (breast) and mucosal versus muscular tissue (colon) (fig. S1C). This suggests that interindividual variance (which partially reflects variation in biospecimen collection) in cell type enrichment driven by tissue heterogeneity is a major determinant in discovery power and benefits iQTL mapping despite being a potential confounding factor for other types of gene expression analyses. Down-sampling analyses in whole blood and transverse colon revealed linear relationships between sample size and ieQTL discovery in these tissues, suggesting that considerably larger numbers of ieQTLs may be discovered with larger sample sizes (fig. S7E). ieQTL discovery was largely robust to the choice of deconvolution method, with ~77% of neutrophil ieQTLs detected with xCell also detected with CIBERSORT, and close to complete replication

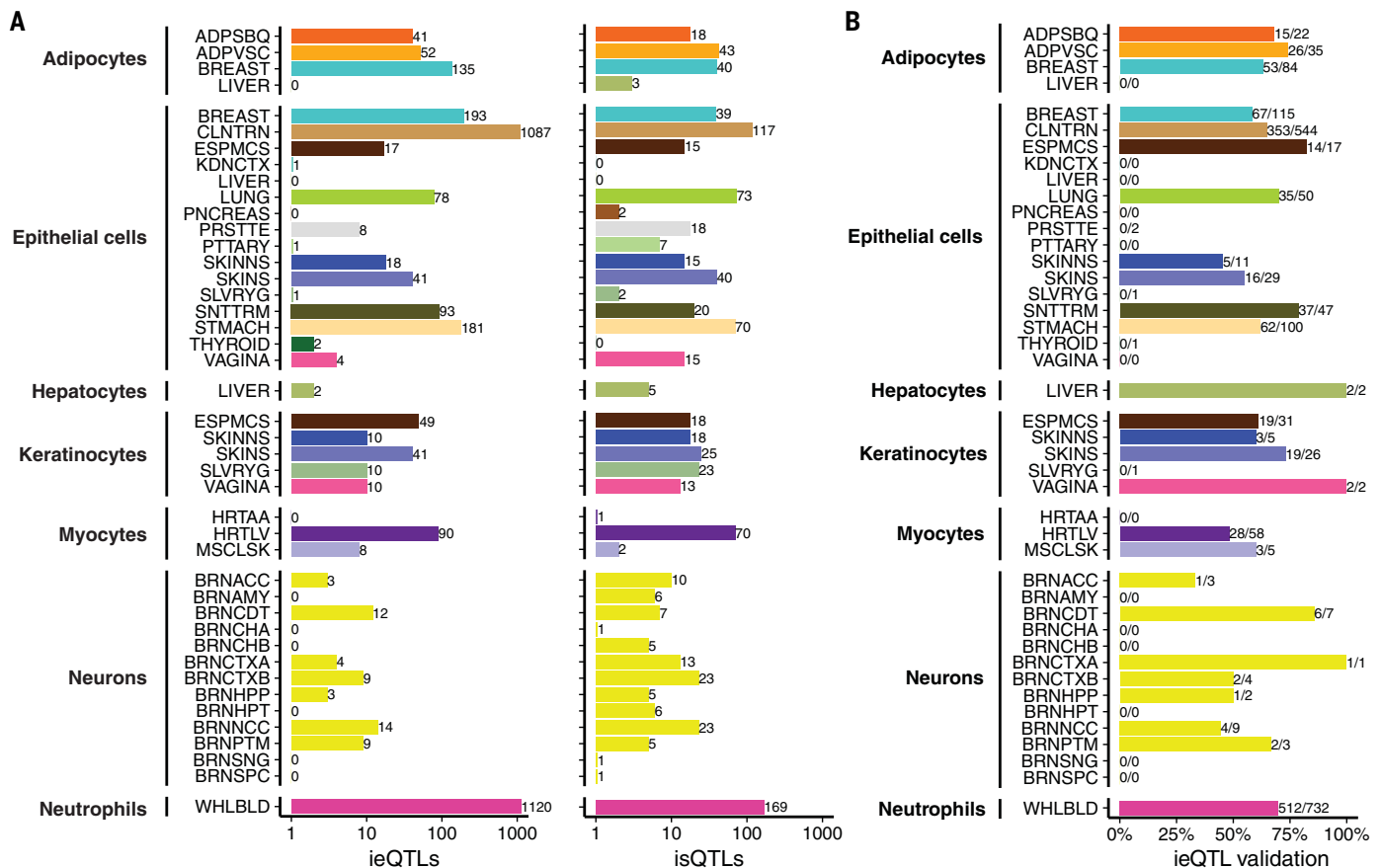


**Fig. 2. Cell type ieQTL and isQTL discovery.** (A) Number of cell type ieQTLs (left) and isQTLs (right) discovered in each cell type–tissue combination at FDR < 5%. Bar labels show the number of ieQTLs and isQTLs, respectively. The color key for the tissues is the same as that of Fig. 1A. (B) Proportion of cell type ieQTLs that validated in ASE data. Validation was defined as ieQTLs for which the Pearson correlation between aFC estimates from ASE and cell type estimates was nominally significant ( $P < 0.05$ ). Tissue abbreviations are provided in table S2. Bar labels indicate the number of ieQTLs with validation per number of ieQTLs tested.

[ $\pi_1 > 0.99$ , where  $\pi_1$  is the proportion of true positives (28)] (fig. S7F).

The QTL effect of ieQTLs and isQTLs can increase or decrease as a function of cell type enrichment (Fig. 1C and fig. S8A). This correlation is usually positive (56%; median across cell type–tissue combinations). As an example, a keratinocyte ieQTL for contactin 1 (*CNTN1*) in skin had a stronger effect in samples with high enrichment of keratinocytes. However, for some ieQTLs the effect was negatively correlated (19%), suggesting that the interaction we identified likely captures an eQTL that is only active in at least one other cell type (fig. S8B). For 24% of ieQTLs, the correlation was ambiguous. At a more stringent FDR cutoff (FDR < 0.01), the median proportion of ieQTLs with ambiguous cell type correlation decreased to 11% (fig. S8B, right), whereas the proportion of ieQTLs with positive correlation increased to 77%. Moreover, the ieQTLs with ambiguous direction tended to have lower minor allele frequency (MAF) (fig. S8C), suggesting that at less stringent FDR, this category might be enriched for false positives.

Altogether, we identified numerous cell type ieQTLs and isQTLs across 43 cell type–tissue combinations, including ieQTLs that are not detected with standard eQTLs analysis in bulk tissue. These cell type ieQTLs pinpoint the cellular specificity of QTLs that might not necessarily be specific to the tested cell type but may also capture eQTL effects of correlated (or anticorrelated) cell types.

#### Validation and replication of cell type ieQTLs

Because few external replication datasets exist, we used allele-specific expression (ASE) data of eQTL heterozygotes (29, 30) to correlate individual-level quantifications of the eQTL effect size [measured as allelic fold-change (aFC)] with individual-level cell type enrichments. If the eQTL is active in the cell type of interest, we expect to see low aFC in individuals with low cell type abundance and higher aFC in individuals with high cell type abundance (fig. S9). The correlation between cell type abundance and aFC across heterozygous individuals can thus be used as a measure of validation for a specific ieQTL.

Using this approach, the median proportion of ieQTLs with a significant ( $P < 0.05$ ) aFC–cell

type Pearson correlation was 0.62 (Fig. 2B). For 13 cell type–tissue combinations with >20 significant ieQTLs, the corresponding  $\pi_1$  statistic (28) confirmed the high validation rate (mean  $\pi_1 = 0.75$ ) (fig. S10). Although this approach does not constitute formal replication in an independent cohort, it is applicable to all tested cell type–tissue combinations and corroborates that ieQTLs are not statistical artifacts of the interaction model.

Next, we performed replication analyses in external cohorts, including whole blood from the GAIT2 study (31), purified neutrophils (9), adipose and skin tissues from the TwinsUK study for ieQTLs (5), and temporal cortex from the Mayo RNA sequencing study for both ieQTLs and isQTLs (32). Replication rates ranged from  $\pi_1 = 0.32$  to 0.67, with the highest rate observed in purified neutrophils for whole blood (fig. S11). The differences in replication rate likely reflect a combination of lower power to detect cell type ieQTLs/isQTLs compared with standard eQTLs/sQTLs, as well as differences in tissue heterogeneity across studies. Taken together, these results show that ieQTLs and isQTLs can be detected with

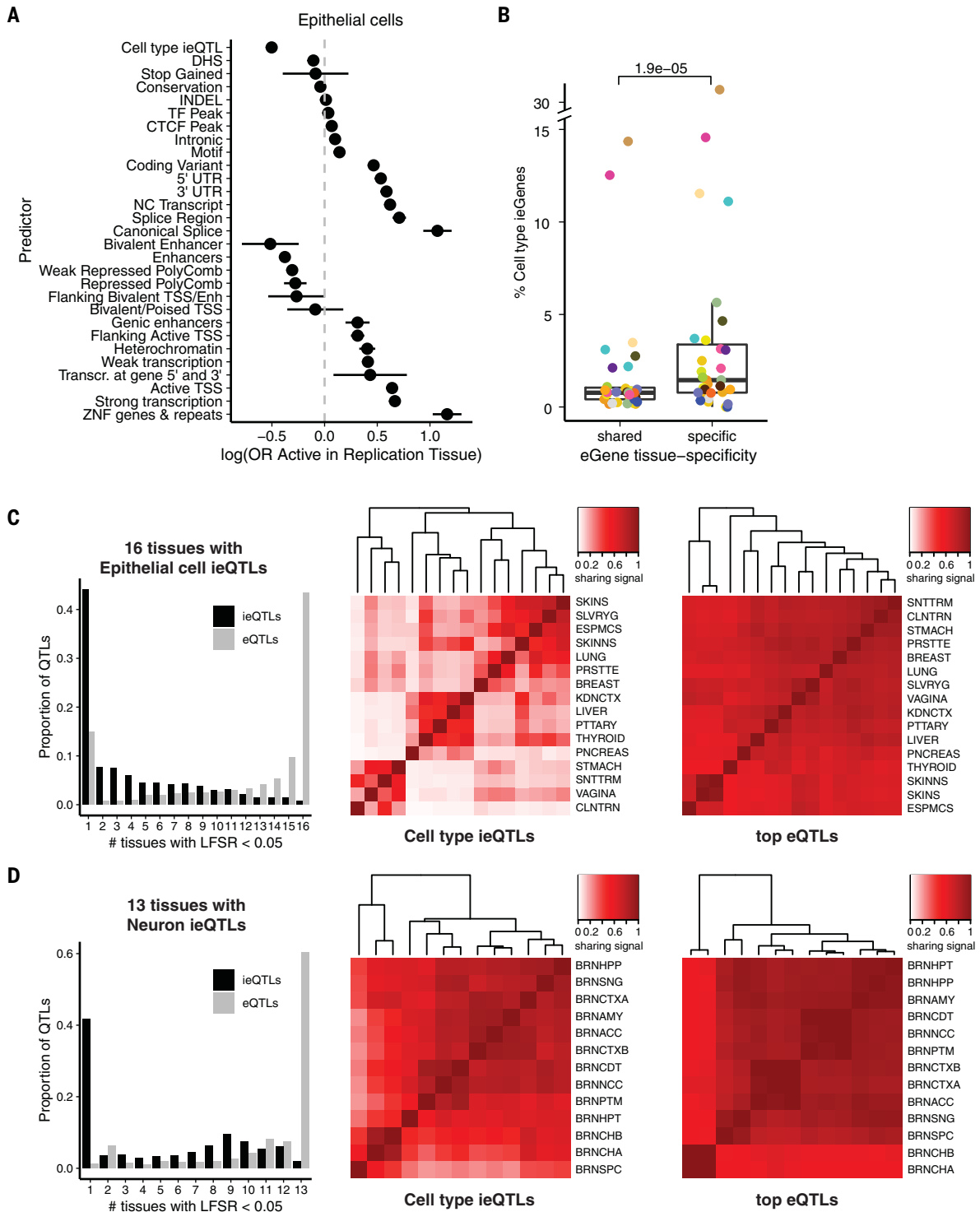


**Fig. 3. Cell type ieQTLs contribute to cis-eQTL tissue specificity.** (A) Coefficients from logistic regression models of cis-eQTL tissue sharing, where epithelial cell ieQTL status is one of the predictors: All significant top cis-eQTLs per tissue were annotated according to whether they were also a significant ieQTL for a given cell type. The coefficients represent the log(odds ratio) that an eQTL is active in a replication tissue given a predictor. Chromatin states were defined by using matched Epigenomics Roadmap tissues and the 15-state ChromHMM (37). Genomic annotations, conservation, and overlaps with Ensembl regulatory build transcription factor (TF), CTCF-binding factor (CTCF), and deoxyribonuclease hypersensitivity site (DHS) peaks are also included. Bars represent the 95% confidence interval.

(B) Proportion of cell type ieQTL genes (ieGenes) among tissue-specific and tissue-shared eGenes. An eGene is considered tissue specific if its eQTL had a MASH LFSR (equivalent to FDR) < 0.05 only in the cell type ieQTL tissue (or tissue type), otherwise it is considered tissue-shared. Results of all 43 cell type-tissue combinations are shown. The color key for the tissues is the same as that of Fig. 1A. (C and D) (Left) Tissue activity of cell type ieQTLs and eQTLs, where a cell type ieQTL and eQTL was considered active in a tissue if it had an LFSR < 0.05. (Middle and right) Pairwise tissue-sharing of (middle) ieQTLs or (right) lead standard cis-eQTLs. The color-coded sharing signal is the proportion of significant QTLs (LFSR < 0.05) that are shared in magnitude (within a factor of 2) and sign between two tissues.

reasonable robustness for diverse cell types and tissues.

### Cell type ieQTLs contribute to tissue specificity

Next, we sought to determine to what extent cell type ieQTLs contribute to the tissue specificity of cis-eQTLs. First, we analyzed ieQTL sharing across cell types, observing that ieQTLs for one cell type were generally not ieQTLs for other cell types (for example, myocyte ieQTLs in muscle tissues were not hepatocyte ieQTLs in liver) (fig. S12A). To determine whether a significant cell type interaction effect is associated with the tissue specificity of an eQTL, we tested whether cell type ieQTLs are predictors of tissue sharing. We annotated the top cis-eQTLs per gene across tissues with their cell type ieQTL status for the five cell types with at least 20 ieQTLs (adipocytes, epithelial cells, keratinocytes, myocytes, and neutrophils). This annotation was included as a predictor in a logistic regression model of eQTL tissue sharing on the basis of eQTL properties, including effect size, minor allele frequency, eGene expression correlation, genomic annotations, and chromatin state (1). In all five cell types, ieQTL

status was a strong negative predictor of tissue sharing, with the magnitude of the effect similar to that of enhancers, indicating that ieQTLs are an important mechanism for tissue-specific regulation of gene expression (Fig. 3A and fig. S12B). Testing whether cell type ieQTLs are predictors of tissue sharing for four cell types with at least 20 isQTLs (adipocytes, epithelial cells, myocytes, and neutrophils) revealed only neutrophil isQTL status as a significant negative predictor (fig. S13). This is likely due to a combination of lower power to detect isQTLs and higher likelihood of splicing-affecting variants having shared effects if a gene is expressed in a tissue or cell type (1).

We corroborated the finding for ieQTLs using multitissue eQTL mapping with MASH (1), testing whether eGenes that are tissue specific [eQTLs discovered at local false sign rate (LFSR) < 0.05 only in the tissue type of interest] have a higher proportion of cell type ieQTLs compared with eGenes that are shared across tissues (LFSR < 0.05 in multiple tissues). The proportion of cell type ieQTLs across all 43 cell type-tissue combinations was significantly higher in tissue-specific eGenes as compared with tissue-shared eGenes ( $P = 1.9 \times 10^{-05}$ , one-sided

Wilcoxon rank sum test) (Fig. 3B), further highlighting the contribution of cell type-specific genetic gene regulation to tissue specificity of eQTLs. For tissues with notably high intersample heterogeneity (such as breast, transverse colon, and stomach), the above-average enrichment is likely at least partially driven by higher power to detect ieQTLs.

To examine the sharing patterns of cell type ieQTLs across tissues, we used two cell types with ieQTLs mapped in >10 tissues (16 tissues for epithelial cells and 13 for neurons). We observed that although standard eQTLs were highly shared across the subsets of 16 and 13 tissues, cell type ieQTLs tended to be highly tissue specific, reflected by an average of four and five tissues with shared ieQTL effects compared with 11 and 12 for eQTLs in epithelial and brain tissues, respectively (Fig. 3, C and D, left). These findings were robust to power differences in detecting eQTLs versus ieQTLs, with eQTLs remaining predominantly shared even when limited to 20% of samples (fig. S14). Of neuron ieQTLs, 25.3% were shared between nine brain tissues, highlighting that tissues of the cerebrum (such as the cortex, basal ganglia, and limbic system) show particularly high levels of sharing

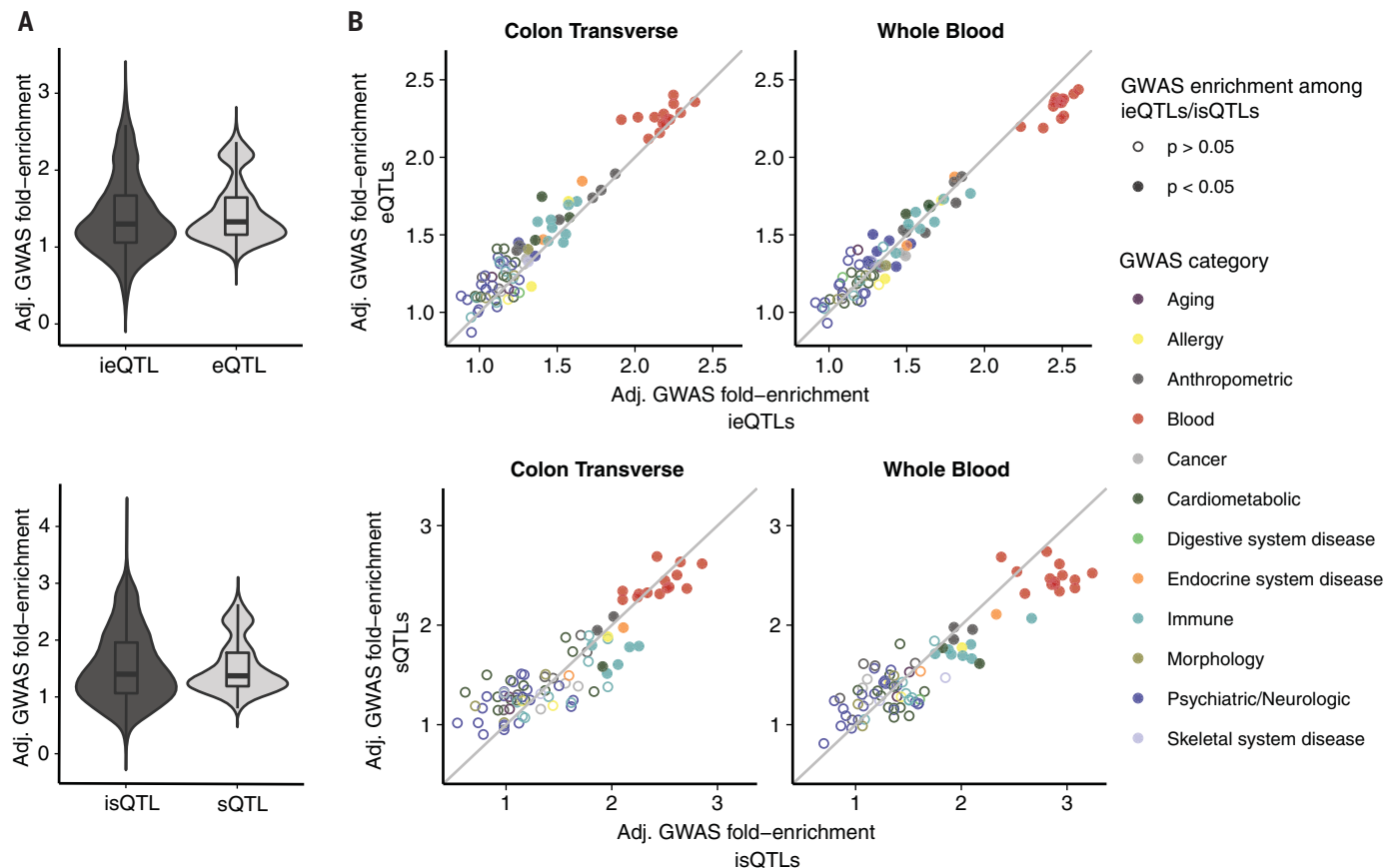


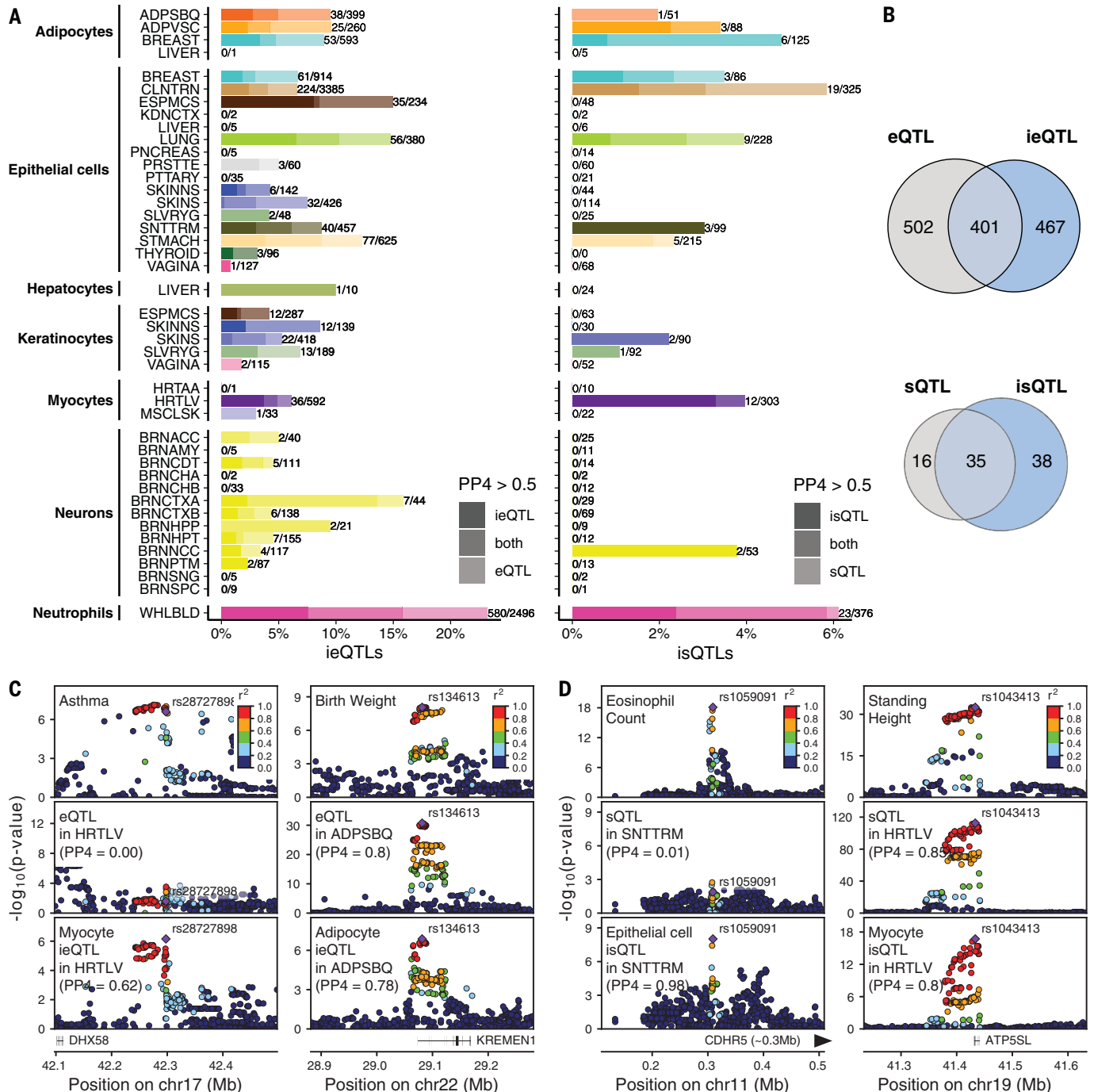
**Fig. 4. Cell type ieQTLs are enriched for GWAS signals.** (A) Distribution of adjusted GWAS fold-enrichment of (top) 23×87 and (bottom) 7×87 tissue-trait combinations using the most significant iQTL or standard QTL per eGene or sGene. (B) Adjusted GWAS fold-enrichments of 87 GWAS traits among iQTLs on the x axis and standard QTLs on the y axis. Solid circles indicate significant GWAS enrichment among iQTLs at  $P < 0.05$  (Bonferroni-corrected). Colors represent GWAS categories of the 87 GWAS traits (table S3).

compared with that of cerebellar tissues, the hypothalamus, and the spinal cord (Fig. 3D, left). This pattern was absent when analyzing standard eQTLs. Pairwise tissue sharing further confirmed that cell type ieQTLs showed greater tissue specificity and more diverse tissue

sharing patterns than those of standard eQTLs, which were broadly shared across all tissues (Fig. 3, C and D, middle and right). These results show that incorporating cell type composition is essential for characterizing the sharing of genetic regulatory effects across tissues.

### GWAS and tissue-specific eQTLs and sQTLs

To study the contribution of cell type–interaction QTLs to genome-wide association study (GWAS) results for 87 complex traits, we first examined the enrichment of ieQTLs of each cell type–tissue combination for trait associations (GWAS,



$P$  values in the *DHX58* locus for (top) an asthma GWAS, (middle) standard heart left ventricle cis-eQTL, and (bottom) myocyte ieQTL, and in the *KREMEN1* locus for a (top) birth weight GWAS, (middle) standard subcutaneous adipose cis-eQTL, and (bottom) adipocyte ieQTL. **(D)** Association  $P$  values in the *CDHR5* locus for (top) an eosinophil count GWAS, (middle) standard small intestine terminal ileum cis-sQTL, and (bottom) epithelial cell isQTL, and in the *ATP5SL* locus for a (top) standing height GWAS, (middle) standard heart left ventricle cis-sQTL, and (bottom) myocyte isQTL.

$P \leq 0.05$ ) using QTLEnrich (33). We used 23 and 7 cell type–tissue pairs (19 and 7 distinct tissues, respectively) with >100 ieQTLs or isQTLs, respectively, at a relaxed FDR of 40% to generate robust enrichment estimates of 87 GWAS traits. Across all tested cell type–tissue trait pairs, the GWAS signal was clearly enriched among ieQTLs and isQTLs (1.3 and 1.4 median fold enrichments, respectively), similarly to standard eQTLs and sQTLs (Fig. 4A and table S4). The GWAS enrichments were robust to the iQTL FDR cutoffs (fig. S15, A and B).

We next analyzed the enrichments of the individual traits for iQTLs of two cell types that we estimated had the largest number of ieQTLs: neutrophil iQTLs in blood and epithelial cell iQTLs in transverse colon. We compared them with the corresponding standard QTLs (Fig. 4B and fig. S15, C and D), focusing on traits that had a significant enrichment for either QTL type (Bonferroni-adjusted  $P < 0.05$ ). In blood, we observed a significant shift toward higher enrichment for ieQTLs (one-sided, paired Wilcoxon rank sum test;  $P = 0.0026$ ) and especially isQTLs ( $P = 2.8 \times 10^{-05}$ ), which appears to be driven by GWAS for blood cell traits, and also immune traits having a higher enrichment for iQTLs. The higher iQTL signal is absent in colon (ieQTL,  $P = 1$ ; isQTL,  $P = 0.13$ ), even though the standard QTL enrichment for blood cell traits appears to be similar for blood and colon. This pattern suggests that cell type–interaction QTLs may have better resolution for indicating relevant tissues and cell types for complex traits as compared with tissue QTLs, but further studies are needed to fully test this hypothesis.

Next, we asked whether cell type iQTLs can be linked to loci discovered in GWASs and used to pinpoint their cellular specificity. To this end, we tested 13,702 ieGenes and 2938 isGenes (40% FDR) for colocalization with 87 GWAS traits (1), using both the cell type ieQTL/isQTL and corresponding standard QTL; 1370 (10.3%) cell type ieQTLs and 89 (3.7%) isQTLs colocalized with at least one GWAS trait (Fig. 5, A and B, and tables S5 and S6). The larger number of colocalizations identified for neutrophil ieQTLs and isQTLs in whole blood relative to other cell type–tissue pairs likely reflects a combination of the larger number of ieQTLs and isQTLs and the abundance of significant GWAS loci for blood-related traits in our set of 87 GWASs (Fig. 5B).

Our analysis revealed a substantial proportion of loci for which only the ieQTL/isQTL colocalizes with the trait (467 of 1370, 34%) (Fig. 5B), or where the joint colocalization of the ieQTL/isQTL and corresponding standard eQTL indicates the cellular specificity of the trait as well as its potential cellular origin (401 of 1370, 29%) (Fig. 5B). For example, a colocalization between the DEXH-box helicase 58 (*DHX58*) gene in the left ventricle of the heart

and an asthma GWAS was only identified through the corresponding myocyte ieQTL [posterior probability of colocalization (PP4) = 0.64] but not the standard eQTL (PP4 = 0.00) (Fig. 5C). Cardiac cells such as cardiomyocytes are not primarily viewed to have a causal role in asthma, but their presence along pulmonary veins and their potential contribution to allergic airway disease have been described (34).

An example in which both the standard eQTL and the cell type ieQTL colocalize with the trait is given in Fig. 5C for *KREMEN1* in adipocytes in subcutaneous adipose tissue and a birth weight GWAS (PP4 ~ 0.8); *KREMEN1* has been linked to adipogenesis in mice (35). We highlight two analogous examples for isQTLs: The epithelial cell isQTL for *CDHR5* in small intestine colocalized with eosinophil counts, whereas the standard sQTL did not (Fig. 5D), and conversely, both the standard sQTL and myocyte ieQTL for *ATP5SL* in the left ventricle of the heart colocalized with standing height (Fig. 5D). Additional examples of ieQTLs and isQTLs colocalizing with trait associations are provided in figs. S16 and S17. Although the iQTLs do not necessarily pinpoint the specific cell type where the regulatory effect is active, they indicate that cell type specificity plays a role in the GWAS locus. Together, our colocalization results indicate that cell type–interaction QTLs yield new potential target genes for GWAS loci that are missed by standard QTLs and provide hypotheses for the cellular specificity of regulatory effects underlying complex traits.

## Discussion

By mapping interaction effects between cell type enrichment and genotype on the transcriptome across GTEx tissues, we provide an atlas of thousands of eQTLs and sQTLs that are likely to be cell type–specific. The ieQTLs and isQTLs we report here include several immune and stromal cell types in tissues where cell type–specific QTLs have not been characterized in prior studies. Cell type ieQTLs are strongly enriched for tissue and cellular specificity and provide a finer resolution to tissue specificity than that of bulk cis-QTLs that are highly shared between tissues. Given the enrichment of GWAS signal in cell type iQTLs for cell types potentially relevant to the traits, and the large fraction of colocalizations with GWAS traits that are only found with cell type iQTLs, exhaustive characterization of cell type–specific QTLs is a highly promising approach toward a mechanistic understanding of these loci, complementing experimental assays of variant function. However, the substantial allelic heterogeneity observed in standard QTLs (1) and limited power to deconvolve QTLs that are specific to rare cell types or with weak or opposing effects indicate that many more cell type–specific QTLs exist beyond those that can be currently computationally inferred from bulk

tissue data. We therefore anticipate that upcoming population-scale single-cell QTL studies will be essential to complement the approaches presented here. However, because those data are still difficult to obtain for many tissues, our demonstration of the insights gained from cell type iQTLs indicates that improving deconvolution approaches and increasing sample sizes will be valuable in this effort and enable discoveries for cell types and tissues not considered in this study.

## Methods summary

The GTEx version 8 (v8) data (1) was used for all analyses. Cell type enrichments were computed with xCell (24). Interaction QTL mapping was performed with tensorQTL (36). Full methods are available in (26).

## REFERENCES AND NOTES

1. GTEx Consortium, The GTEx Consortium atlas of genetic regulatory effects across human tissues. *Science* **369**, 1318 (2020).
2. U. Vösa *et al.*, Unraveling the polygenic architecture of complex traits using blood eQTL meta-analysis. *bioRxiv* 447367 [Preprint] 19 October 2018. doi: [10.1101/447367](https://doi.org/10.1101/447367)
3. R. Joehanes *et al.*, Integrated genome-wide analysis of expression quantitative trait loci aids interpretation of genomic association studies. *Genome Biol.* **18**, 16 (2017). doi: [10.1186/s13059-016-1142-6](https://doi.org/10.1186/s13059-016-1142-6); pmid: 28122634
4. H. Kirsten *et al.*, Dissecting the genetics of the human transcriptome identifies novel trait-related trans-eQTLs and corroborates the regulatory relevance of non-protein coding loci. *Hum. Mol. Genet.* **24**, 4746–4763 (2015). doi: [10.1093/hmg/ddv194](https://doi.org/10.1093/hmg/ddv194); pmid: 26019233
5. A. Buil *et al.*, Gene-gene and gene-environment interactions detected by transcriptome sequence analysis in twins. *Nat. Genet.* **47**, 88–91 (2015). doi: [10.1038/ng.3162](https://doi.org/10.1038/ng.3162); pmid: 25436857
6. GTEx Consortium, The Genotype-Tissue Expression (GTEx) pilot analysis: Multitissue gene regulation in humans. *Science* **348**, 648–660 (2015). doi: [10.1126/science.1262110](https://doi.org/10.1126/science.1262110); pmid: 25954001
7. B. P. Fairfax *et al.*, Genetics of gene expression in primary immune cells identifies cell type-specific master regulators and roles of HLA alleles. *Nat. Genet.* **44**, 502–510 (2012). doi: [10.1038/ng.2205](https://doi.org/10.1038/ng.2205); pmid: 22446964
8. T. Raj *et al.*, Polarization of the effects of autoimmune and neurodegenerative risk alleles in leukocytes. *Science* **344**, 519–523 (2014). doi: [10.1126/science.1249547](https://doi.org/10.1126/science.1249547); pmid: 24786080
9. V. Naranbhai *et al.*, Genomic modulators of gene expression in human neutrophils. *Nat. Commun.* **6**, 7545 (2015). doi: [10.1038/ncomms8545](https://doi.org/10.1038/ncomms8545); pmid: 26151758
10. S. Kim-Hellmuth *et al.*, Genetic regulatory effects modified by immune activation contribute to autoimmune disease associations. *Nat. Commun.* **8**, 266 (2017). doi: [10.1038/s41467-017-00366-1](https://doi.org/10.1038/s41467-017-00366-1); pmid: 28814792
11. S. Kasela *et al.*, Pathogenic implications for autoimmune mechanisms derived by comparative eQTL analysis of CD4<sup>+</sup> versus CD8<sup>+</sup> T cells. *PLoS Genet.* **13**, e1006643–e21 (2017). doi: [10.1371/journal.pgen.1006643](https://doi.org/10.1371/journal.pgen.1006643); pmid: 28248954
12. M. G. P. van der Wijst *et al.*, Single-cell RNA sequencing identifies celltype-specific cis-eQTLs and co-expression QTLs. *Nat. Genet.* **50**, 493–497 (2018). doi: [10.1038/s41588-018-0089-9](https://doi.org/10.1038/s41588-018-0089-9); pmid: 29610479
13. N. Habib *et al.*, Massively parallel single-nucleus RNA-seq with DroNc-seq. *Nat. Methods* **14**, 955–958 (2017). doi: [10.1038/nmeth.4407](https://doi.org/10.1038/nmeth.4407); pmid: 28846088
14. M. Slyper *et al.*, A single-cell and single-nucleus RNA-seq toolbox for fresh and frozen human tumors. *Nat. Med.* **26**, 792–802 (2020). doi: [10.1038/s41591-020-0844-1](https://doi.org/10.1038/s41591-020-0844-1); pmid: 32405060
15. HCA Consortium, The Human Cell Atlas. *arXiv:1810.05192* [q-bio.TO] (2018).
16. A. K. Sarkar *et al.*, Discovery and characterization of variance QTLs in human induced pluripotent stem cells. *PLoS Genet.* **15**, e1008045–e16 (2019). doi: [10.1371/journal.pgen.1008045](https://doi.org/10.1371/journal.pgen.1008045); pmid: 31002671



17. I. Mandric *et al.*, Optimal design of single-cell RNA sequencing experiments for cell-type-specific eQTL analysis. *bioRxiv* 766972 [Preprint] 12 September 2019. doi: [10.1101/766972](https://doi.org/10.1101/766972)
18. M. G. P. van der Wijst *et al.*, Science Forum: The single-cell eQTLGen consortium. *eLife* **9**, e25155 (2020).
19. H.-J. Westra *et al.*, Cell Specific eQTL Analysis without Sorting Cells. *PLoS Genet.* **11**, e1005223–e17 (2015). doi: [10.1371/journal.pgen.1005223](https://doi.org/10.1371/journal.pgen.1005223); pmid: 25955312
20. D. V. Zhernakova *et al.*, Identification of context-dependent expression quantitative trait loci in whole blood. *Nat. Genet.* **49**, 139–145 (2017). doi: [10.1038/ng.3737](https://doi.org/10.1038/ng.3737); pmid: 27918533
21. C. A. Glastonbury, A. Couto Alves, J. S. El-Sayed Moustafa, K. S. Small, Cell-Type Heterogeneity in Adipose Tissue Is Associated with Complex Traits and Reveals Disease-Relevant Cell-Specific eQTLs. *Am. J. Hum. Genet.* **104**, 1013–1024 (2019). doi: [10.1016/j.ajhg.2019.03.025](https://doi.org/10.1016/j.ajhg.2019.03.025); pmid: 31130283
22. F. Avila Cobos, J. Vandesompele, P. Mestdagh, K. De Preter, Computational deconvolution of transcriptomics data from mixed cell populations. *Bioinformatics* **34**, 1969–1979 (2018). doi: [10.1093/bioinformatics/bty019](https://doi.org/10.1093/bioinformatics/bty019); pmid: 29351586
23. G. Sturm *et al.*, Comprehensive evaluation of transcriptome-based cell-type quantification methods for immuno-oncology. *Bioinformatics* **35**, i436–i445 (2019). doi: [10.1093/bioinformatics/btz363](https://doi.org/10.1093/bioinformatics/btz363); pmid: 31510660
24. D. Aran, Z. Hu, A. J. Butte, xCell: Digitally portraying the tissue cellular heterogeneity landscape. *Genome Biol.* **18**, 220 (2017). doi: [10.1186/s13059-017-1349-1](https://doi.org/10.1186/s13059-017-1349-1); pmid: 29141660
25. Y. I. Li *et al.*, Annotation-free quantification of RNA splicing using LeafCutter. *Nat. Genet.* **50**, 151–158 (2018). doi: [10.1038/s41588-017-0004-9](https://doi.org/10.1038/s41588-017-0004-9); pmid: 29229983
26. See supplementary materials.
27. A. Breschi *et al.*, A limited set of transcriptional programs define major cell types. *Genome Res.* **30**, 1047–1059 (2020).
28. J. D. Storey, R. Tibshirani, Statistical significance for genome-wide studies. *Proc. Natl. Acad. Sci. U.S.A.* **100**, 9440–9445 (2003). doi: [10.1073/pnas.1530509100](https://doi.org/10.1073/pnas.1530509100); pmid: 12883005
29. S. E. Castel *et al.*, A vast resource of allelic expression data spanning human tissues. *Genome Res.* **10.1186/s13059-020-02122-z** (2020).
30. P. Mohammadi, S. E. Castel, A. A. Brown, T. Lappalainen, Quantifying the regulatory effect size of cis-acting genetic variation using allelic fold change. *Genome Res.* **27**, 1872–1884 (2017). doi: [10.1101/gr.216747.116](https://doi.org/10.1101/gr.216747.116); pmid: 29021289
31. L. Vila *et al.*, Heritability of thromboxane A2 and prostaglandin E2 biosynthetic machinery in a Spanish population. *Arterioscler. Thromb. Vasc. Biol.* **30**, 128–134 (2010). doi: [10.1161/ATVBAHA.109.193219](https://doi.org/10.1161/ATVBAHA.109.193219); pmid: 19850905
32. M. Allen *et al.*, Human whole genome genotype and transcriptome data for Alzheimer's and other neurodegenerative diseases. *Sci. Data* **3**, 160089 (2016). doi: [10.1038/sdata.2016.89](https://doi.org/10.1038/sdata.2016.89); pmid: 27727239
33. E. R. Gamazon *et al.*, Using an atlas of gene regulation across 44 human tissues to inform complex disease- and trait-associated variation. *Nat. Genet.* **50**, 956–967 (2018). doi: [10.1038/s41588-018-0154-4](https://doi.org/10.1038/s41588-018-0154-4); pmid: 29955180
34. S. S. Folsom, C. J. Gottardi, Cardiomyocytes of the heart and pulmonary veins: Novel contributors to asthma? *Am. J. Respir. Cell Mol. Biol.* **57**, 512–518 (2017). doi: [10.1165/rcmb.2016-0261TR](https://doi.org/10.1165/rcmb.2016-0261TR); pmid: 28481622
35. C. Christodoulides *et al.*, The Wnt antagonist Dickkopf-1 and its receptors are coordinately regulated during early human adipogenesis. *J. Cell Sci.* **119**, 2613–2620 (2006). doi: [10.1242/jcs.02975](https://doi.org/10.1242/jcs.02975); pmid: 16763196
36. A. Taylor-Weiner *et al.*, Scaling computational genomics to millions of individuals with GPUs. *Genome Biol.* **20**, 228 (2019). doi: [10.1186/s13059-019-1836-7](https://doi.org/10.1186/s13059-019-1836-7); pmid: 31675989
37. J. Ernst, M. Kellis, Chromatin-state discovery and genome annotation with ChromHMM. *Nat. Protoc.* **12**, 2478–2492 (2017). doi: [10.1038/nprot.2017.124](https://doi.org/10.1038/nprot.2017.124); pmid: 29120462

## ACKNOWLEDGMENTS

We thank the donors and their families for their generous gifts of organ donation for transplantation, and tissue donations for the GTEx research project; we thank M. Khan for the illustrations in Fig. 1A. **Funding:** This work was funded by following funding sources: Marie-Skłodowska Curie fellowship H2020 grant 706636 (S.K.-H.); NIH grant 1K99HG009916-01 (S.E.C.); NIH grant R01HG002585 (G.W. and M.S.); B102015-70777-P, Ministerio de Economía y Competitividad and FEDER funds (M.M.-A., V.W., R.G., and D.G.-M.); FPU15/03635, Ministerio de Educación, Cultura y Deporte (M.M.-A.); "la Caixa" Foundation (ID 100010434) agreement

LCF/BQ/SO15/52260001 (D.G.-M.); EU IMI program (UE7-DIRECT-115317-1) (A.V. and E.T.D.); FNS-funded project RNA1 (31003A\_149984) (A.V. and E.T.D.); Massachusetts Lions Eye Research Fund Grant (A.R.H.); MRC grants MR/R023131/1 and MR/M004422/1 (K.S.S.); and Biomedical Big Data Training Grant 5T32LM012424-03 (B.N.). The TwinsUK study was funded by the Wellcome Trust and European Community's Seventh Framework Programme (FP7/2007-2013). The TwinsUK study also receives support from the National Institute for Health Research (NIHR)-funded BioResource, Clinical Research Facility and Biomedical Research Centre based at Guy's and St Thomas' NHS Foundation Trust in partnership with King's College London. This work was further supported by the Common Fund of the Office of the Director, U.S. National Institutes of Health (NIH), and by NCI, NHGRI, NHLBI, NIDA, NIMH, NIA, NIAID, and NINDS through NIH contracts HHSN261200800001E (Leidos Prime contract with NCI: A.M.S., D.E.T., N.V.R., J.A.M., L.S., M.E.B., L.Q., T.K., D.B., K.R., and A.U.), 10XS170 (NDRI: W.F.L., J.A.T., G.K., A.M., S.S., R.H., G.Wa., M.J., M.Wa., L.E.B., C.J., J.W., B.R., M.Hu., K.M., L.A.S., H.M.G., M.Mo., and L.K.B.), 10XS171 (Roswell Park Cancer Institute: B.A.F., M.T.M., E.K., B.M.G., K.D.R., and J.B.), 10X172 (Science Care), 12ST1039 (IDOX), 10ST1035 (Van Andel Institute: S.D.J., D.C.R., and D.R.V.), HHSN268201000029C (Broad Institute: F.A., G.G., K.G.A., A.V.S., X.Li, E.T., S.G., A.G., S.A., K.H.H., D.T.N., K.H., S.R.M., and J.L.N.), 5U41HG009494 (F.A., G.G., and K.G.A.), and through NIH grants R01 DA006227-17 (University of Miami Brain Bank: D.C.M. and D.A.D.), R01 MH090941 (University of Geneva), R01 MH090951 and R01 MH090937 (University of Chicago), R01 MH090936 (University of North Carolina-Chapel Hill), R01MH101814 (M.M.-A., V.W., S.B.M., R.G., E.T.D., D.G.-M., and A.V.), U01HG007593 (S.B.M.), R01MH101822 (C.D.B.), U01HG007598 (M.O. and B.E.S.), U01MH104393 (A.P.F.). Extension H002371 to 5U41HG002371 (W.J.K.) as well as other funding sources: R01MH106842 (T.L., P.M., E.F., and P.J.H.), R01HL142028 (T.L., SiKa., and P.J.H.), R01GM122924 (T.L. and S.E.C.), R01MH107666 (H.K.I.), P30DK020595 (H.K.I.), U01HG008901 (T.L.), R01GM124486 (T.L.), R01HG1010067 (Y.Pa.), R01HG002585 (G.Wa. and M.St.), Gordon and Betty Moore Foundation GBMF 4559 (G.Wa. and M.St.), R01HG006855 (Se.Ka., R.E.H.), NIH CTSA grant UL1TR002550-01 (P.M.), R35HG101718 (E.R.G.), R01MH109905, R01HG100480 (A.Ba.), Searle Scholar Program (A.Ba.), R01HG008150 (S.B.M.), 5T32HG000044-22, NHGRI Institutional Training Grant in Genome Science (N.R.G.), and F32HG009987 (F.H.). **Author contributions:** S.K.-H., F.A., and T.L. conceived the study. S.K.-H. and F.A. led the writing, figure generation, and editing of the manuscript and supplementary materials. S.K.-H. coordinated analyses of all contributing authors; S.K.-H. and F.A. generated pipelines and performed iQTL mapping; S.K.-H., F.A., M.O., M.M.-A., V.W., D.G.-M., S.M., B.N., and J.Q. performed cell type benchmarking analyses; S.K. performed iQTL validation with ASE data using the validation pipeline and ASE data generated by S.E.C.; F.A., A.V., and A.L.R. performed replication analyses; S.E.C. performed QTL tissue activity prediction analysis; S.K.-H. and S.E.C. generated tissue sharing (MASH) data; S.K.-H. performed tissue specificity, multi-tissue analysis, and colocalization analysis; A.R.H. performed QTL enrichment analysis; G.W. and Y.Z. provided software support for multi-tissue eQTL analysis; X.W. and H.K.I. provided advice on colocalization analysis; A.B., A.M.-P., and J.M.-S. contributed to replication analysis; F.A. and K.G.A. generated and oversaw GTEx v8 data generation, LDACC, pipelines; A.N.B. and R.B. generated GWAS data; K.S.S., M.S., H.S.X., G.G., E.T.D., H.K.I., R.G., A.V.S., B.E.S., K.G.A., and T.L. supervised the work of trainees in their laboratories; and M.O. and T.L. contributed to editing of the manuscript. All authors read and approved the final manuscript. **Competing interests:** F.A. is an inventor on a patent application related to TensorQTL; S.E.C. is a cofounder, chief technology officer, and stock owner at Variant Bio; J.Q. is an employee of Pfizer; H.S.X. is an employee of AbbVie; H.K.I. has received speaker honoraria from GSK and AbbVie; E.T.D. is chairman and member of the board of Hybridstat; G.G. receives research funds from IBM and Pharmacytics and is an inventor on patent applications related to MuTect, ABSOLUTE, MutSig, MSMuTect, MSMutSig, POLYSOLVER, and TensorQTL. G.G. is a founder, consultant, and holds privately held equity in Scorpion Therapeutics; T.L. is a scientific advisory board member of Variant Bio with equity and Goldfinch Bio. GTEx consortium members: P.F. is member of the scientific advisory boards of Fabric Genomics and Eagle Genomes. P.G.F. is a partner of Bioinf2Bio. E.R.G. is on the Editorial Board of Circulation Research and does consulting for the City of Hope/Beckman Research Institute; B.E.E. is on the scientific advisory boards of Celsius Therapeutics and Freenome; S.B.M. is on the scientific advisory board of Prime Genomics; D.G.M. is a cofounder with equity in Goldfinch Bio and has received research support from AbbVie, Astellas, Biogen, BioMarin,

Eisai, Merck, Pfizer, and Sanofi-Genzyme. **Data and materials availability:** All GTEx open-access data, including summary statistics and visualizations of cell type iQTLs, are available on the GTEx Portal (<https://gtexportal.org/home/datasets>). All GTEx protected data are available via dbGaP (accession phs000424.v8). Access to the raw sequence data are now provided through the AnVil platform (<https://gtexportal.org/home/protectedDataAccess>). Eighty-seven harmonized and imputed GWAS summary stats described in table S3 are available and linked at <https://github.com/hakylimlab/gtex-gwas-analysis> and <https://zenodo.org/record/3629742#XxYGoylh0Ux>. Original GWAS studies are cited in (1). The QTL mapping pipeline is available at <https://github.com/broadinstitute/gtex-pipeline> and <https://doi.org/10.5281/zenodo.3727189>, and tensorQTL is available at <https://github.com/broadinstitute/tensorqtl> and <https://doi.org/10.5281/zenodo.3726360>. Residual GTEx biospecimens have been banked and remain available as a resource for further studies (access can be requested on the GTEx Portal, at [www.gtexportal.org/home/samplesPage](http://www.gtexportal.org/home/samplesPage)).

## SUPPLEMENTARY MATERIALS

[science.sciencemag.org/content/369/6509/eaaz8528/suppl/DC1](https://science.sciencemag.org/content/369/6509/eaaz8528/suppl/DC1)

Materials and Methods

Figs. S1 to S17

References (38–62)

Tables S1 to S6

[View/request a protocol for this paper from Bio-protocol.](#)

## GTEx Consortium

### Laboratory and Data Analysis Coordinating Center (LDACC):

Francois Aguet<sup>1</sup>, Shankara Anand<sup>1</sup>, Kristin G. Ardlie<sup>2</sup>, Stacey Gabriel<sup>3</sup>, Gad A. Getz<sup>2,3</sup>, Aaron Grubert<sup>1</sup>, Kane Hadley<sup>4</sup>, Robert E. Handsaker<sup>4,5,6</sup>, Katherine H. Huang<sup>7</sup>, Seva Kashin<sup>4,5,6</sup>, Xiao Li<sup>1</sup>, Daniel G. MacArthur<sup>4,7</sup>, Samuel R. Meier<sup>1</sup>, Jared L. Nedzfel<sup>1</sup>, Duyen T. Nguyen<sup>1</sup>, Ayellet V. Segre<sup>1,8</sup>, Ellen Todres<sup>1</sup>

### Analysis Working Group (funded by GTEx project grants):

Francois Aguet<sup>1</sup>, Shankara Anand<sup>1</sup>, Kristin G. Ardlie<sup>2</sup>, Brunilda Balliu<sup>9</sup>, Alvaro N. Barbeira<sup>10</sup>, Alexis Battle<sup>11,12</sup>, Rodrigo Bonazzola<sup>10</sup>, Andrew Brown<sup>13,14</sup>, Christopher D. Brown<sup>15</sup>, Stephane E. Castel<sup>16,17</sup>, Donald F. Conrad<sup>18,19</sup>, Daniel J. Cotter<sup>20</sup>, Nancy Cox<sup>21</sup>, Sayantan Das<sup>22</sup>, Olivia M. de Goede<sup>20</sup>, Emmanouil T. Dermizakis<sup>13,23,24</sup>, Jonah Einson<sup>16,25</sup>, Barbara E. Engelhardt<sup>26,27</sup>, Eleazar Eskin<sup>28</sup>, Tiffany Y. Eulalio<sup>29</sup>, Nicole M. Ferraro<sup>29</sup>, Elise D. Flynn<sup>16,17</sup>, Laure Fresard<sup>30</sup>, Eric R. Gamazon<sup>21,31,32,33</sup>, Diego Garrido-Martín<sup>34</sup>, Nicole R. Gay<sup>20</sup>, Gad A. Getz<sup>2,3</sup>, Michael J. Gloudemans<sup>29</sup>, Aaron Grubert<sup>1</sup>, Roderic Guigó<sup>34,35</sup>, Kane Hadley<sup>4</sup>, Andrew R. Hame<sup>8,1</sup>, Robert E. Handsaker<sup>4,5,6</sup>, Yuan He<sup>11</sup>, Paul J. Hoffman<sup>16</sup>, Farhad Hormozdizadeh<sup>1,36</sup>, Lei Hou<sup>1,37</sup>, Katherine H. Huang<sup>7</sup>, Hae Kyung Im<sup>10</sup>, Brian Jo<sup>26,27</sup>, Silva Kasela<sup>16,17</sup>, Seva Kashin<sup>4,5,6</sup>, Manolis Kellis<sup>1,37</sup>, Sarah Kim-Hellmuth<sup>16,17,38</sup>, Alan Kwong<sup>22</sup>, Tuuli Lappalainen<sup>16,17</sup>, Xiao Li<sup>1</sup>, Xin Li<sup>30</sup>, Yanyu Liang<sup>10</sup>, Daniel G. MacArthur<sup>4,7</sup>, Sergei Mangul<sup>28,39</sup>, Samuel R. Meier<sup>1</sup>, Pejman Mohammadi<sup>16,17,40,41</sup>, Stephen B. Montgomery<sup>20,30</sup>, Manuel Muñoz-Aguirre<sup>34,42</sup>, Daniel C. Natchun<sup>10</sup>, Jared L. Nedzfel<sup>1</sup>, Duyen T. Nguyen<sup>1</sup>, Andrew B. Nobel<sup>43</sup>, Merikell Oliva<sup>10,44</sup>, YoSon Park<sup>15,45</sup>, Yongjin Park<sup>1,37</sup>, Princy Parsana<sup>42</sup>, Abhiram S. Rao<sup>46</sup>, Ferran Reverter<sup>47</sup>, John M. Rouhana<sup>1,8</sup>, Chiara Sabatti<sup>48</sup>, Ashis Saha<sup>12</sup>, Ayellet V. Segre<sup>1,8</sup>, Andrew D. Skol<sup>10,49</sup>, Matthew Stephens<sup>50</sup>, Barbara E. Stranger<sup>10,51</sup>, Benjamin J. Strober<sup>11</sup>, Nicole A. Teran<sup>30</sup>, Ellen Todres<sup>1</sup>, Ana Viñuela<sup>13,23,24,52</sup>, Gao Wang<sup>50</sup>, Xiaoque Wen<sup>22</sup>, Fred Wright<sup>53</sup>, Valentin Wucher<sup>34</sup>, Yuxin Zou<sup>34</sup>

### Analysis Working Group (not funded by GTEx project grants):

Pedro G. Ferreira<sup>55,56,57,58</sup>, Gen Li<sup>59</sup>, Marta Melé<sup>60</sup>, Esti Yeger-Lotem<sup>61,62</sup>

**Leidos Biomedical—project management:** Mary E. Barcus<sup>63</sup>, Debra Bradbury<sup>63</sup>, Tanya Krubitz<sup>63</sup>, Jeffrey A. McLean<sup>63</sup>, Liqun Qi<sup>63</sup>, Karna Robinson<sup>63</sup>, Nancy V. Roche<sup>63</sup>, Anna M. Smith<sup>63</sup>, Leslie Sobin<sup>63</sup>, David E. Tabor<sup>63</sup>, Anita Undale<sup>63</sup>

**Biospecimen collection source sites:** Jason Bridge<sup>64</sup>, Lori E. Brigham<sup>65</sup>, Barbara A. Foster<sup>66</sup>, Bryan M. Gillard<sup>66</sup>, Richard Hasz<sup>67</sup>, Marcus Hunter<sup>68</sup>, Christopher Johns<sup>69</sup>, Mark Johnson<sup>70</sup>, Ellen Karasik<sup>66</sup>, Gene Kopen<sup>71</sup>, William F. Leinweber<sup>71</sup>, Alisha McDonald<sup>71</sup>, Michael T. Moser<sup>66</sup>, Kevin Myer<sup>68</sup>, Kimberley D. Ramsey<sup>66</sup>, Brian Roe<sup>68</sup>, Saboor Shad<sup>71</sup>, Jeffrey A. Thomas<sup>71,70</sup>, Gary Walters<sup>70</sup>, Michael Washington<sup>70</sup>, Joseph Wheeler<sup>69</sup>

**Biospecimen core resource:** Scott D. Jewell<sup>72</sup>, Daniel C. Rohrer<sup>72</sup>, Dana R. Valley<sup>72</sup>

### Brain bank repository:

David A. Davis<sup>73</sup>, Deborah C. Mash<sup>73</sup>

### Pathology:

Mary E. Barcus<sup>63</sup>, Philip A. Branton<sup>74</sup>, Leslie Sobin<sup>63</sup>

### ELSI Study:

Laura K. Barker<sup>75</sup>, Heather M. Gardiner<sup>75</sup>

### Genome browser data integration and visualization:

Paul Flicek<sup>76</sup>, Maximilian Haeussler<sup>78</sup>, Thomas Juettemann<sup>77</sup>, W. James Kent<sup>78</sup>, Christopher M. Lee<sup>78</sup>, Conner C. Powell<sup>78</sup>,

Kate R. Rosenbloom<sup>78</sup>, Magali Ruffier<sup>77</sup>, Dan Sheppard<sup>77</sup>, Kieron Taylor<sup>77</sup>, Stephen J. Trevanion<sup>77</sup>, Daniel R. Zerbino<sup>77</sup>  
**eGTEx groups:** Nathan S. Abell<sup>20</sup>, Joshua Akey<sup>79</sup>, Lin Chen<sup>44</sup>, Kathryn Demanelis<sup>44</sup>, Jennifer A. Doherty<sup>80</sup>, Andrew P. Feinberg<sup>81</sup>, Kasper D. Hansen<sup>82</sup>, Peter F. Hickey<sup>83</sup>, Lei Hou<sup>1,37</sup>, Farzana Jasmine<sup>44</sup>, Lihua Jiang<sup>20</sup>, Rajinder Kaur<sup>84,85</sup>, Manolis Kellis<sup>1,37</sup>, Muhammad G. Kibriya<sup>44</sup>, Jin Billy Li<sup>20</sup>, Qin Li<sup>20</sup>, Shin Lin<sup>86</sup>, Sandra E. Linder<sup>20</sup>, Stephen B. Montgomery<sup>20,30</sup>, Meritxell Oliva<sup>10,44</sup>, Yongjin Park<sup>1,37</sup>, Brandon L. Pierce<sup>44</sup>, Lindsay F. Rizzardi<sup>87</sup>, Andrew D. Skol<sup>10,49</sup>, Kevin S. Smith<sup>30</sup>, Michael Snyder<sup>20</sup>, John Stamatoyannopoulos<sup>84,88</sup>, Barbara E. Stranger<sup>10,51</sup>, Hua Tang<sup>20</sup>, Meng Wang<sup>20</sup>

**NIH program management:** Philip A. Branton<sup>74</sup>, Latarsha J. Carithers<sup>74,89</sup>, Ping Guan<sup>74</sup>, Susan E. Koester<sup>90</sup>, A. Roger Little<sup>91</sup>, Helen M. Moore<sup>74</sup>, Concepcion R. Nierras<sup>92</sup>, Abhi K. Rao<sup>74</sup>, Jimmie B. Vaught<sup>74</sup>, Simona Volpi<sup>93</sup>

<sup>1</sup>Broad Institute of MIT and Harvard, Cambridge, MA, USA. <sup>2</sup>Cancer Center and Department of Pathology, Massachusetts General Hospital, Boston, MA, USA. <sup>3</sup>Harvard Medical School, Boston, MA, USA. <sup>4</sup>Department of Genetics, Harvard Medical School, Boston, MA, USA. <sup>5</sup>Program in Medical and Population Genetics, Broad Institute of MIT and Harvard, Cambridge, MA, USA. <sup>6</sup>Stanley Center for Psychiatric Research, Broad Institute of MIT and Harvard, Cambridge, MA, USA. <sup>7</sup>Analytic and Translational Genetics Unit, Massachusetts General Hospital, Boston, MA, USA. <sup>8</sup>Ocular Genomics Institute, Massachusetts Eye and Ear, Harvard Medical School, Boston, MA, USA. <sup>9</sup>Department of Biomathematics, University of California, Los Angeles, CA, USA. <sup>10</sup>Section of Genetic Medicine, Department of Medicine, The University of Chicago, Chicago, IL, USA. <sup>11</sup>Department of Biomedical Engineering, Johns Hopkins University, Baltimore, MD, USA. <sup>12</sup>Department of Computer Science, Johns Hopkins University, Baltimore, MD, USA. <sup>13</sup>Department of Genetic Medicine and Development, University of Geneva Medical School, Geneva, Switzerland. <sup>14</sup>Population Health and Genomics, University of Dundee, Dundee, Scotland, UK. <sup>15</sup>Department of Genetics, University of Pennsylvania, Perelman School of Medicine, Philadelphia, PA, USA. <sup>16</sup>New York Genome Center, New York, NY, USA. <sup>17</sup>Department of Systems Biology, Columbia University, New York, NY, USA. <sup>18</sup>Department of Genetics, Washington University School of Medicine, St. Louis, MO, USA. <sup>19</sup>Division of Genetics, Oregon National Primate Research Center, Oregon Health & Science University, Portland, OR, USA. <sup>20</sup>Department of Genetics, Stanford University, Stanford, CA, USA. <sup>21</sup>Division of Genetic Medicine, Department of Medicine, Vanderbilt University Medical Center, Nashville, TN, USA. <sup>22</sup>Department of Biostatistics, University of Michigan, Ann Arbor, MI, USA. <sup>23</sup>Institute for Genetics and Genomics in Geneva (IGEG), University of Geneva, Geneva, Switzerland. <sup>24</sup>Swiss Institute of Bioinformatics, Geneva, Switzerland. <sup>25</sup>Department of Biomedical Informatics, Columbia

University, New York, NY, USA. <sup>26</sup>Department of Computer Science, Princeton University, Princeton, NJ, USA. <sup>27</sup>Center for Statistics and Machine Learning, Princeton University, Princeton, NJ, USA. <sup>28</sup>Department of Computer Science, University of California, Los Angeles, CA, USA. <sup>29</sup>Program in Biomedical Informatics, Stanford University School of Medicine, Stanford, CA, USA. <sup>30</sup>Department of Pathology, Stanford University, Stanford, CA, USA. <sup>31</sup>Data Science Institute, Vanderbilt University, Nashville, TN, USA. <sup>32</sup>Clare Hall, University of Cambridge, Cambridge, UK. <sup>33</sup>MRC Epidemiology Unit, University of Cambridge, Cambridge, UK. <sup>34</sup>Centre for Genomic Regulation (CRG), The Barcelona Institute for Science and Technology, Barcelona, Catalonia, Spain. <sup>35</sup>Universitat Pompeu Fabra (UPF), Barcelona, Catalonia, Spain. <sup>36</sup>Department of Epidemiology, Harvard T.H. Chan School of Public Health, Boston, MA, USA. <sup>37</sup>Computer Science and Artificial Intelligence Laboratory, Massachusetts Institute of Technology, Cambridge, MA, USA. <sup>38</sup>Statistical Genetics, Max Planck Institute of Psychiatry, Munich, Germany. <sup>39</sup>Department of Clinical Pharmacy, School of Pharmacy, University of Southern California, Los Angeles, CA, USA. <sup>40</sup>Scripps Research Translational Institute, La Jolla, CA, USA. <sup>41</sup>Department of Integrative Structural and Computational Biology, The Scripps Research Institute, La Jolla, CA, USA. <sup>42</sup>Department of Statistics and Operations Research, Universitat Politècnica de Catalunya (UPC), Barcelona, Catalonia, Spain. <sup>43</sup>Department of Statistics and Operations Research and Department of Biostatistics, University of North Carolina, Chapel Hill, NC, USA. <sup>44</sup>Department of Public Health Sciences, The University of Chicago, Chicago, IL, USA. <sup>45</sup>Department of Systems Pharmacology and Translational Therapeutics, Perelman School of Medicine, University of Pennsylvania, Philadelphia, PA, USA. <sup>46</sup>Department of Bioengineering, Stanford University, Stanford, CA, USA. <sup>47</sup>Department of Genetics, Microbiology and Statistics, University of Barcelona, Barcelona, Spain. <sup>48</sup>Departments of Biomedical Data Science and Statistics, Stanford University, Stanford, CA, USA. <sup>49</sup>Department of Pathology and Laboratory Medicine, Ann & Robert H. Lurie Children's Hospital of Chicago, Chicago, IL, USA. <sup>50</sup>Department of Human Genetics, University of Chicago, Chicago, IL, USA. <sup>51</sup>Center for Genetic Medicine, Department of Pharmacology, Northwestern University, Feinberg School of Medicine, Chicago, IL, USA. <sup>52</sup>Department of Twin Research and Genetic Epidemiology, King's College London, London, UK. <sup>53</sup>Bioinformatics Research Center and Departments of Statistics and Biological Sciences, North Carolina State University, Raleigh, NC, USA. <sup>54</sup>Department of Statistics, University of Chicago, Chicago, IL, USA. <sup>55</sup>Department of Computer Sciences, Faculty of Sciences, University of Porto, Porto, Portugal. <sup>56</sup>Instituto de Investigação e Inovação em Saúde, University of Porto, Porto, Portugal. <sup>57</sup>Institute of Molecular Pathology and Immunology, University of Porto, Porto, Portugal. <sup>58</sup>Laboratory of Artificial Intelligence and Decision Support, Institute for Systems and Computer Engineering,

Technology and Science, Porto, Portugal. <sup>59</sup>Mailman School of Public Health, Columbia University, New York, NY, USA. <sup>60</sup>Life Sciences Department, Barcelona Supercomputing Center, Barcelona, Spain. <sup>61</sup>Department of Clinical Biochemistry and Pharmacology, Ben-Gurion University of the Negev, Beer-Sheva, Israel. <sup>62</sup>National Institute for Biotechnology in the Negev, Beer-Sheva, Israel. <sup>63</sup>Leidos Biomedical, Rockville, MD, USA. <sup>64</sup>Upstate New York Transplant Services, Buffalo, NY, USA. <sup>65</sup>Washington Regional Transplant Community, Annandale, VA, USA. <sup>66</sup>Therapeutics, Roswell Park Comprehensive Cancer Center, Buffalo, NY, USA. <sup>67</sup>Gift of Life Donor Program, Philadelphia, PA, USA. <sup>68</sup>LifeGift, Houston, TX, USA. <sup>69</sup>Center for Organ Recovery and Education, Pittsburgh, PA, USA. <sup>70</sup>LifeNet Health, Virginia Beach, VA, USA. <sup>71</sup>National Disease Research Interchange, Philadelphia, PA, USA. <sup>72</sup>Van Andel Research Institute, Grand Rapids, MI, USA. <sup>73</sup>Department of Neurology, University of Miami Miller School of Medicine, Miami, FL, USA. <sup>74</sup>Biorepositories and Biospecimen Research Branch, Division of Cancer Treatment and Diagnosis, National Cancer Institute, National Institutes of Health, Bethesda, MD, USA. <sup>75</sup>College of Public Health, Temple University, Philadelphia, PA, USA. <sup>76</sup>Virginia Commonwealth University, Richmond, VA, USA. <sup>77</sup>European Molecular Biology Laboratory, European Bioinformatics Institute, Hinxton, UK. <sup>78</sup>Genomics Institute, University of California, Santa Cruz, CA, USA. <sup>79</sup>Carl Icahn Laboratory, Princeton University, Princeton, NJ, USA. <sup>80</sup>Department of Population Health Sciences, The University of Utah, Salt Lake City, UT, USA. <sup>81</sup>Departments of Medicine, Biomedical Engineering, and Mental Health, Johns Hopkins University, Baltimore, MD, USA. <sup>82</sup>Department of Biostatistics, Bloomberg School of Public Health, Johns Hopkins University, Baltimore, MD, USA. <sup>83</sup>Department of Medical Biology, The Walter and Eliza Hall Institute of Medical Research, Parkville, Victoria, Australia. <sup>84</sup>Altius Institute for Biomedical Sciences, Seattle, WA, USA. <sup>85</sup>Division of Genetics, University of Washington, Seattle, WA, USA. <sup>86</sup>Department of Cardiology, University of Washington, Seattle, WA, USA. <sup>87</sup>HudsonAlpha Institute for Biotechnology, Huntsville, AL, USA. <sup>88</sup>Genome Sciences, University of Washington, Seattle, WA, USA. <sup>89</sup>National Institute of Dental and Craniofacial Research, National Institutes of Health, Bethesda, MD, USA. <sup>90</sup>Division of Neuroscience and Basic Behavioral Science, National Institute of Mental Health, National Institutes of Health, Bethesda, MD, USA. <sup>91</sup>National Institute on Drug Abuse, Bethesda, MD, USA. <sup>92</sup>Office of Strategic Coordination, Division of Program Coordination, Planning and Strategic Initiatives, Office of the Director, National Institutes of Health, Rockville, MD, USA. <sup>93</sup>Division of Genomic Medicine, National Human Genome Research Institute, Bethesda, MD, USA.

14 October 2019; accepted 31 July 2020  
 10.1126/science.aaz8528

## Cell type–specific genetic regulation of gene expression across human tissues

Sarah Kim-Hellmuth, François Aguet, Meritxell Oliva, Manuel Muñoz-Aguirre, Silva Kasela, Valentin Wucher, Stephane E. Castel, Andrew R. Hamel, Ana Viñuela, Amy L. Roberts, Serghei Mangul, Xiaoquan Wen, Gao Wang, Alvaro N. Barbeira, Diego Garrido-Martín, Brian B. Nadel, Yuxin Zou, Rodrigo Bonazzola, Jie Quan, Andrew Brown, Angel Martinez-Perez, José Manuel Soria, GTEx Consortium, Gad Getz, Emmanouil T. Dermitzakis, Kerrin S. Small, Matthew Stephens, Hualin S. Xi, Hae Kyung Im, Roderic Guigó, Ayellet V. Segre, Barbara E. Stranger, Kristin G. Ardlie and Tuuli Lappalainen

*Science* **369** (6509), eaaz8528.  
DOI: 10.1126/science.aaz8528

### Cell type–specific quantitative trait loci

Understanding how human genetic variation affects phenotype requires tissue- or even cell type–specific measurements. Kim-Hellmuth *et al.* used computational methods to identify cell-type proportions within bulk tissues in the Genotype-Tissue Expression (GTEx) project dataset to identify cell-type interaction quantitative trait loci and map these to genetic variants correlated with expression or splicing differences between individuals. By characterizing the cellular context, this study illustrates how genetic variants that operate in a cell type–specific manner affect gene regulation and can be linked to complex traits. This deconvolution and analysis of cell types from bulk tissues allows greater precision in understanding how phenotypes are linked to genetic variation.

*Science*, this issue p. eaaz8528

#### ARTICLE TOOLS

<http://science.sciencemag.org/content/369/6509/eaaz8528>

#### SUPPLEMENTARY MATERIALS

<http://science.sciencemag.org/content/suppl/2020/09/09/369.6509.eaaz8528.DC1>

#### RELATED CONTENT

<http://science.sciencemag.org/content/sci/369/6509/eaba3066.full>  
<http://science.sciencemag.org/content/sci/369/6509/1318.full>  
<http://science.sciencemag.org/content/sci/369/6509/1316.full>  
<http://science.sciencemag.org/content/sci/369/6509/eaaz5900.full>  
<http://science.sciencemag.org/content/sci/369/6509/eaaz6876.full>

#### REFERENCES

This article cites 61 articles, 14 of which you can access for free  
<http://science.sciencemag.org/content/369/6509/eaaz8528#BIBL>

#### PERMISSIONS

<http://www.sciencemag.org/help/reprints-and-permissions>

Use of this article is subject to the [Terms of Service](#)

---

*Science* (print ISSN 0036-8075; online ISSN 1095-9203) is published by the American Association for the Advancement of Science, 1200 New York Avenue NW, Washington, DC 20005. The title *Science* is a registered trademark of AAAS.

Copyright © 2020 The Authors, some rights reserved; exclusive licensee American Association for the Advancement of Science. No claim to original U.S. Government Works